Static concentrating photovoltaic modelling using MATLAB

To cite this article: Firdaus Muhammad-Sukki *et al* 2021 *J. Phys.: Conf. Ser.* **2053** 012003

View the article online for updates and enhancements.

You may also like

Static concentrating photovoltaic modelling using MATLAB

**Firdaus Muhammad-Sukki [1,2, *], Haroon Farooq [3], Siti Hawa Abu-Bakar [4],
Jorge Alfredo Ardila-Rey [5], Nazmi Sellami [6], Ciaran Kilpatrick [6],
Mohd Nabil Muhtazaruddin [2], Nurul Aini Bani [2] and Muhammad Zulkipli [7]**

[1] Edinburgh Napier University, United Kingdom
[2] Universiti Teknologi Malaysia, Malaysia
[3] University of Engineering and Technology, Pakistan
[4] Universiti Kuala Lumpur, Malaysia
[5] Universidad Técnica Federico Santa María, Chile
[6] Robert Gordon University, United Kingdom
[7] Universiti Tun Hussein Onn Malaysia, Malaysia

* Corresponding author's email : f.muhammadsukki@napier.ac.uk

Abstract. The world has recorded an increasing interest and staggering investment in renewable technology in the last two decades, specifically in solar photovoltaic (PV). Concentrating PV (CPV) is one of PV's technology advancements and is gaining popularity for integration in a building. Various CPV designs are currently being investigated by researchers. The aim of this paper is to design and develop a MATLAB programme that can predict the electrical properties of a static concentrator that is designed with a $\pm 40°$ acceptance angle. The programme was utlizied to determine the angular characteristics of the static concentrator between acceptance angle of -50° and 50°. It is proposed that the optoelectronic gain, $C_{\text{opto-e}}$ values be incorporated into the model to simulate a CPV design. The incident angle values (within $\pm 50°$) were chosen to demonstrate that the static concentrator could collect solar energy within its designed acceptance angle of $\pm 40°$. The current-voltage and power-voltage characteristics are generated for each simulation, and critical parameters such as the maximum power, open-circuit voltage, short-circuit current, and optoelectronic gain were identified and measured. The programme was found to be able to determine the electrical properties for the static concentrator.

1. Introduction

Solar photovoltaic (PV) technology has drawn major investment and research interest since the early 2000s, with the focus on improving the effectiveness of solar photovoltaic cells and addressing the economy feasibility of producing energy with the solar technology. The interaction of light photons with electrons in a solar cell that gives rise to the photovoltaic effect, primarily constructed of a doped semiconductor, mainly silicon to produce a p-n junction, is the working principle of the solar PV system. The electrons within the junction are freed as a result of this interaction, resulting in a hole to be occupied by any free electron moving in the p-n junction. With a constant supply of light source, these electrons contacts aggregate, resulting in an electron flow and, thus producing current. A commercially available solar cell made from silicon typically generates 0.5–0.6 V with resulting current of 28–35 mA/cm^2 [1]. For practical application, solar cells are grouped to form solar panels, allowing the generation of solar energy, and solar arrays are built by combining these panels, offering a more extensive surface area and generating much more electricity.

One way to improve the efficiency of a solar panel is by increasing the irradiance of sun energy that arrive at the surface area of the solar cell. This can be achieved through the use of a solar concentrator. If properly configured, a solar panel can be built with a relatively less number of solar cells than a regular solar panel of equal surface area would require [2]. The concentrating PV (CPV) technique is the name for this method. Furthermore, depending on the geometry of these lenses, the panel may absorb a large fraction of sun energy, even when it is not precisely oriented towards the light source, enhancing its efficiency even further in comparison to a regular solar panel.

With the advancement of PV systems, the world is seeing a growing demand to estimate solar PV performance and anticipate the total amount of energy produced under a particular set of conditions. Consequently, equivalent circuits for PV cells and other mathematical models have been developed to forecast a PV cell's performance characteristics and possible output power. It is worth noting that these models are not identical; each one has its own set of parameters. Experiments are frequently used to confirm the efficiency of these models.

Li et al. [3] detailed the development and testing of a MATLAB simulation for obtaining the model's parameters utilising open circuit currents, closed circuit currents, and maximum power, via an iterative calculation until convergence. The models' performance were compared to the projected features from the datasheet of the PV cells and experimental findings of different PV modules, yielding an average inaccuracy of 5.53%. Mahmoud et al. [4] thoroughly presented the design and testing of a new method for calculating PV cell parameters using the data provided within the manufacturer's datasheet and the single-diode equivalent circuit. When tested against experimental results, it had a normalised root mean square deviation of less than 4.91%, and for most tests, the error was around 1%, therefore, making this an excellent mathematical simulation model.

Mehta et al. [5] designed and implemented a single-diode model using MATLAB to tackle the noise in the measurements and results in a highly accurate model where the errors recorded were between 2.5938×10^{-5} and 1.6299×10^{-3} A when compared with experimental results. Vinod et al. [6] created a single-diode model using MATLAB/Simulink. Their stepwise model requires three parameters to be identified analytically, namely the photocurrent, the saturation current and the reverse saturation current. The simulation results achieved a maximum relative error of 1.65% when compared with the experimental result.

This work seeks to forecast the current-voltage (I-V) and power-voltage (P-V) characteristics of a static concentrator. The following is how the paper is organised: Section 1 provides an overview of the static concentrator and solar photovoltaic modelling, Section 2 details the processes to model the concentrator's features, Section 4 shows the findings from the bespoke model, and Section 5 concludes.

2. Modelling of the static concentrator

This study uses analytical methods in the MATLAB programming environment to offer a modelling of a single-diode equivalent circuit for a CPV configuration. When Vinod et al. [6] used Simulink to model a solar PV module, they provided a stepwise technique, which is used in this model. During modelling, the datasheet for a solar PV cell from National Renewable Energy Centre was used, as well as results from earlier studies characterising the static concentrator. Simulation-generated characteristics of I-V and P-V are examined to experiment-derived values.

Ramirez-Iniguez et al. [7] designed the static concentrator to enhance electrical yield, reducing the amount of expensive PV material used, lowering the PV system's cost [8]. Ramirez-Iniguez et al. [7] have provided a detailed description of the static concentrator creation process. It is proposed that the value of optoelectronic gain should be incorporated in the modelling of any CPV. All CPV concentrates sun energy from a vast region into a smaller concentrated area where a solar PV cell is installed [9]. Equation 1 shows the relationship between the solar irradiance, G, with the irradiance at reference of 1,000 W/m^2, G_{ref}, the optoelectronic gain, C_{opto-e} as well as the angle of incidence with the integration of CPV, G_{con}. C_{opto-e} is equivalent to 1 for a non-CPV.

$$G_{con} = C_{opto-e} \left(\frac{G}{G_{ref}}\right) \cos\theta \qquad (1)$$

Muhammad-Sukki et al. presented their indoor tests to characterise the static concentrator-PV configuration in [10]. The static concentrator is 3 cm in height and has a 1 cm^2 square exit aperture area. It also has a geometrical concentration gain of 4.91. Along its x-axis, the concentrator is designed to attain a half-acceptance angle of ±40 degrees. At varied incidence angles between -50 degrees and 50 degrees, the angular response of the static concentrator -PV configuration and the plain PV cell was examined. The angular response allows the static concentrator's optoelectronic gain to be measured at various incidence angles. The static concentrator's optoelectronic gain at various incidence angles is presented in the following Table 1.

Table 1. The static concentrator's optoelectronic gain at various angles of incidence.

The Angle of Incidence (˚)	Opto-electronic Gain, C_{opto-e}
0	4.17143
±5	4.00000
±10	3.89205
±15	3.60465
±20	3.37313
±25	3.14642
±30	2.78105
±35	1.84722
±40	1.21561
±45	0.95142
±50	0.69643

A solar PV cell's current and voltage output can be predicted by converting it to an equivalent electrical circuit. A diode coupled in parallel with a photocurrent, I_{ph}, is ideal for representing a PV cell's equivalent circuit as a light generated current source. However, in practice, factors such as the material's resistivity, the influence of shunt resistance and the ohmic losses must all be considered. Series resistance, R_s and shunt resistance, R_{sh} are two factors that can be simulated. The PV cell's equivalent circuit can be represented using a single-diode model. Equation (2) [11] gives the following formula for the output current of a single-diode model:

$$I = I_{ph} - I_d - I_{sh} \tag{2}$$

where I_d is the diode currents. Equation (1) can be expressed as [12]:

$$I = I_{ph} - I_s \left[\exp\left(\frac{q(V + IR_s)}{n_d kT} - 1\right)\right] - \frac{V + IR_s}{R_{sh}} \tag{3}$$

where I_s is the diode's saturation current, n_d is the diode ideality factor, q is the electron charge (1.602 x 10^{-19} C), k is the Boltzman constant (1.38 x 10^{-23} J/K), T is the p-n junction temperature (in Kelvin), and V is the the PV cell's voltage.

It is necessary to calculate I_s, I_{ph}, and I_{rs} in this model. The following equations will be used to calculate the values. I_{ph} is unaffected by V (or R_s), is linearly dependent on solar irradiation, and is temperature-dependent. Equation 4 [6] illustrates this link.

$$I_{ph} = (I_{sc} + \alpha(T - T_{ref})) * G_{con} \tag{4}$$

where T_{ref} is 25 ˚C and α is the current temperature coefficient.

Saturation current I_s and reverse saturation current, I_{rs} are calculated using both Equations (5) and (6), with the value of the energy bandgap, E_g, as reported by Vinod et al. [6]. The essential parameters values of the solar PV cell are listed in Table 2. The solar PV cell's manufacturer, Narec, gave these parameters (National Renewable Energy Centre).

$$I_{rs} = I_{sc} / \left[\exp\left(\frac{qV_{oc}}{n_{d1}kT}\right) - 1 \right] \tag{5}$$

$$I_s = I_{rs} \left[\frac{T}{T_{ref}}\right]^3 \exp\left[\left(\frac{qE_g}{n_d k}\right)\left(\frac{1}{T} - \frac{1}{T_{ref}}\right)\right] \tag{6}$$

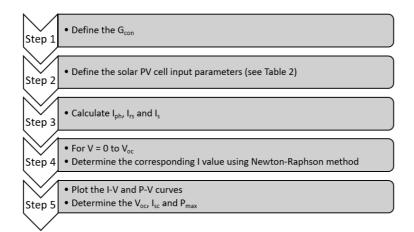**Table 2.** Essential parameters of the solar cell

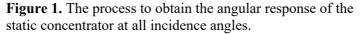| Component	Value
Solar radiation intensity, G_{ref}	1,000 W/m^2
Reference Temperature, T_{ref}	25 ˚C
Square solar cell area, A	1 cm^2
Short circuit current, I_{sc} (at 0˚)	0.0350 A
Open-circuit voltage, V_{oc} (at 0˚)	0.586 V
Ideality factor, n	1.109
Energy bandgap, E_g	1.12
Charge of an electron, q	1.6 x 10^{-19} C
Boltzman constant, k	1.38 x 10^{-23} m^2 kg s^{-2} K^{-1}
Series resistance, R_s	0.047994 Ω
Shunt resistance, R_{sh}	2148.53 Ω
Short circuit current temperature coefficient, α	0.00024 A/˚C

3. Simulation process

Equation (1)- was used to create a MATLAB algorithm to simulate the electrical power output generated by the static concentrator-PV construction (6). The code was created to emulate the static concentrator-PV configuration's angular properties from -50 degrees to 50 degrees with a 5 degrees increment. Figure 1 shows the stages involved in creating the I-V and P-V curves for each incident angle. The solar beams are perpendicular to the static concentrator at a 0 incidence angle. The incident angle range (±50 degrees) was chosen to show that the static concentrator can capture solar rays within its acceptance angle of ±40 degrees. The code considers a number of factors, including solar irradiation, optoelectronic gain (as shown in Equation (1)), and the solar PV cell's key characteristics. The values of I_{ph}, I_{rs}, and I_s are then calculated analytically by the programme. The equivalent I value for voltages that range from 0 to V_{oc} is then derived using the Newton- Raphson iteration method by substituting Equations (4)–(6) into Equation (3). P is derived by multiplying the matching values of I and V. Finally, the I-V and P-V curves are plotted. The I-V and P-V characteristics were produced in each simulation, and maximum power (P_{max}), the short circuit current (I_{sc}), open-circuit voltage (V_{oc}), and optoelectronic gain (C_{opto-e}) were calculated and recorded.
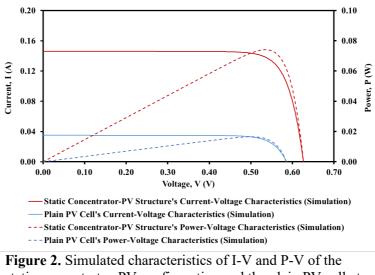
Step 1 • Define the G_{con}

Step 2 • Define the solar PV cell input parameters (see Table 2)

Step 3 • Calculate I_{ph}, I_{rs} and I_s

Step 4 • For V = 0 to V_{oc}
• Determine the corresponding I value using Newton-Raphson method

Step 5 • Plot the I-V and P-V curves
• Determine the V_{oc}, I_{sc} and P_{max}

Figure 1. The process to obtain the angular response of the static concentrator at all incidence angles.

4. Results and discussions

The simulated characteristics of I-V and P-V for the static concentrator -PV configuration and a plain PV cell at normal incidence were run at a temperature of 25 °C with sun irradiation of 1,000 W/m^2 as shown in Figure 3. According to calculations, the plain PV cell produced the maximum power output of 0.0165 W, open-circuit voltage of 0.5860 V, and short circuit current of 0.0350 A. The addition of static concentrator boosts the maximum output power to 0.0740 W, the open-circuit voltage to 0.0627 V, and the short circuit voltage to 0.1460 A. A value of 4.1714 is calculated as the simulated optoelectronic gain.

Static Concentrator-PV Structure's Current-Voltage Characteristics (Simulation)
Plain PV Cell's Current-Voltage Characteristics (Simulation)
Static Concentrator-PV Structure's Power-Voltage Characteristics (Simulation)
Plain PV Cell's Power-Voltage Characteristics (Simulation)

Figure 2. Simulated characteristics of I-V and P-V of the static concentrator-PV configuration and the plain PV cell at STCs at normal incidence.

In order to analyse the angular response of the static concentrator-PV configuration and the plain PV cell, it was tested at various incidence angles ranging from -50 degree to 50 degree at STCs. Each simulation determined and recorded the maximum power, short circuit current, open-circuit voltage, and optoelectronic gain.

Figure 3 shows the simulated short circuit currents of the static concentrator-PV configuration and a plain PV cell at different incidence angles. The short circuit current for the static concentrator-PV configuration dropped from 0.1460 A at average to 0.1219 A at ±15° of incidence. When the incident

angle is greater than ±30°, the short circuit current dropped to less than half of its highest value. Outside of the intended half-acceptance angle of 40, the static concentrator-PV configuration produces a lower short circuit current than a plain PV cell. Moreover, these rays escaped through the side profile of the concentrator and did not reach the exit aperture at angles outside of the half-acceptance angle. Instead, they emitted through the concentrator's side profile [13]. Within the 'design' half-acceptance angles, the static concentrator-PV configuration provides a considerably larger short circuit current than a plain PV cell. As the incident angle increases from 0° to ±50°, the plain PV cell shows a similar trend, with the simulated short circuit current at normal incidence drops from 0.0350 A to lower values.
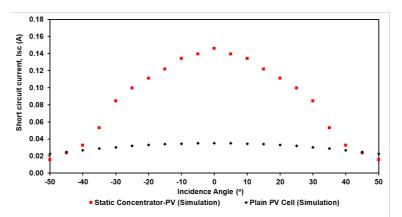

Figure 3. The simulated short circuit currents for the static concentrator-PV configuration and a plain PV cell at STCs.

Figures 4 demonstrates the simulated open-circuit voltages generated for the static concentrator-PV configuration vs a plain PV cell for various angles of incidence at STCs. For the static concentrator-PV configuration at normal incidence, the value of open circuit voltage gradually decreased from 0.6270 V to 0.5440 V at a ±50 degrees angle of incidence. Meanwhile, the corresponding value for the plain PV cell at normal incidence gradually decreased from 0.5860 V to 0.5740 V at a ±50 degrees angle of incidence.
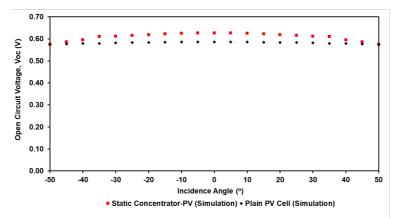

Figure 4. Comparison of the simulated open circuit voltages for the static concentrator-PV configuration and a plain PV cell at STCs.

Figure 5 compares the numbers derived from simulations for the static concentrator-PV configuration with a plain PV cell at STCs for different incident angles at maximum power generation. According to simulations, the max value of 0.0740 W was attained at normal incidence for the static concentrator-PV configuration. At a ±15 degrees angle of incidence, the value dropped to 0.0613 W. However, as the incident angle becomes greater than ±30 degrees, the maximum power value drops to lower than 50%

of the maximum value. Outside of the design half-acceptance angle of 40 degrees, the maximum power value generated by the static concentrator-PV configuration is lower than that produced by a plain PV cell. The plain PV cell exhibits a similar trend, where the corresponding value drops from 0.0165 W at normal incidence to lesser values when the incident angle is increased from 0 to ±50 degrees.
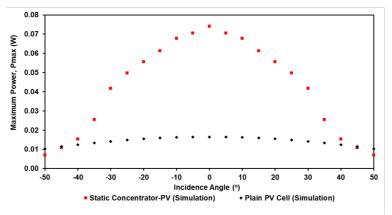

Figure 5. Comparison of the simulated maximum powers for the static concentrator-PV configuration and a plain PV cell at STCs.

Figure 6 displays the optoelectronic gains for the static concentrator-PV configuration at STCs based on simulations. The simulated optoelectronic gain decreased from a peak of 4.1714 at normal incidence to 3.6047 at a ±15 degrees angle of incidence. When the incident angle exceeds ±30 degrees, the optoelectronic gain value drops to lower than 50% of its maximum value. Beyond the design of half-acceptance angle of ±40 degrees, the optoelectronic gain value is less than 1.
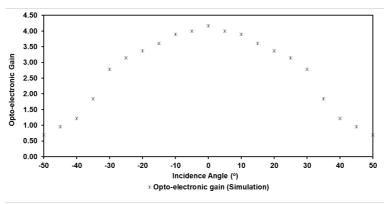

Figure 6. Simulated optoelectronic gains for the static concentrator-PV configuration at STCs.

5. Conclusions

Modelling the performance and predicting the energy generated by any solar PV cell has become increasingly popular. As a result, several researchers have constructed equivalent circuits for PV cells and other modellings to forecast the characteristics and possible photovoltaic cell output power. The performance of a MATLAB algorithm created to model the I-V as well as P-V properties of the static concentrator-PV configuration was discussed in this work. Under STCs, the static concentrator-PV configuration and the plain PV cell are simulated at various incidence angles that ranges from -50 degrees to 50 degrees. The simulations produced an excellent result, allowing the short-circuit current values, open circuit voltage, maximum power, and optoelectronic gain to be calculated. The model's accuracy would be determined by comparing the simulations to the experimental results.

6. References

[1] Qazi S 2017 Mobile Photovoltaic Systems for Disaster Relief and Remote Areas *Standalone Photovoltaic (PV) Systems for Disaster Relief and Remote Areas* (Massachusetts, USA: Elsevier) pp 83–112

[2] Alamoudi A, Saaduddin S M, Munir A B, Muhammad-Sukki F, Abu-Bakar S H, Mohd Yasin S H, Karim R, Bani N A, Mas'ud A A, Ardila-Rey J A, Prabhu R and Sellami N 2019 Using static concentrator technology to achieve global energy goal *Sustainability* **11** 3056:1-22

[3] Li W, Paul M C, Baig H, Siviter J, Montecucco A, Mallick T K and Knox A R 2019 A three-point-based electrical model and its application in a photovoltaic thermal hybrid roof-top system with crosed compound parabolic concentrator *Renew. Energy* **130** 400–15

[4] Mahmoud Y A, Xiao W and Zeineldin H H 2013 A parameterisation approach for enhancing PV model accuracy *IEEE Trans. Ind. Electron.* **60** 5708–16

[5] Mehta H K, Warke H, Kukadiya K and Panchal A K 2019 Accurate Expressions for Single-Diode-Model Solar Cell Parameterization *IEEE J. Photovoltaics* **9** 803–10

[6] Vinod, Kumar R and Singh S K 2018 Solar photovoltaic modeling and simulation: As a renewable energy solution *Energy Reports* **4** 701–12

[7] Ramirez-iniguez R, Muhammad-Sukki F, McMeekin S G and Stewart B G 2018 Optical element (Patent No. US9,910,253,B2) 1–26

[8] Muhammad-Sukki F, Abu-Bakar S H, Ramirez-Iniguez R, McMeekin S G, Stewart B G, Sarmah N, Mallick T K, Munir A B, Mohd Yasin S H and Abdul Rahim R 2014 Mirror symmetrical dielectric totally internally reflecting concentrator for building integrated photovoltaic systems *Appl. Energy* **113** 32–40

[9] O'Gallagher J J 2008 Nonimaging Optics in Solar Energy *Synth. Lect. Energy Environ. Technol. Sci. Soc.* **2** 1–120

[10] Muhammad-Sukki F, Abu-Bakar S H, Ramirez-Iniguez R, McMeekin S G, Stewart B G, Munir A B, Mohd Yasin S H and Abdul Rahim R 2013 Performance analysis of a mirror symmetrical dielectric totally internally reflecting concentrator for building integrated photovoltaic systems *Appl. Energy* **111** 288–99

[11] Bonkoungou D, Koalaga Z and Njomo D 2013 Modelling and simulation of photovoltaic module considering single-diode equivalent circuit model in MATLAB *Int. J. Emerg. Technol. Adv. Eng.* **3** 493–502

[12] Mammo E D, Sellami N and Mallick T K 2013 Performance analysis of a reflective 3D crossed compound parabolic concentrating photovoltaic system for building façade integration *Prog. Photovoltaics Res. Appl.* **21** 1095–103

[13] Welford W T and Winston R 1989 *High Collection Nonimaging Optics* (California, USA: Academic Press)